

UCSF

UC San Francisco Previously Published Works

Title

Association Between Biochemical Markers of Bone Turnover and Bone Changes on Imaging: Data From the Osteoarthritis Initiative

Permalink

<https://escholarship.org/uc/item/4sj5d7jk>

Journal

Arthritis Care & Research, 69(8)

ISSN

2151-464X

Authors

Deveza, Leticia A
Kraus, Virginia B
Collins, Jamie E
[et al.](#)

Publication Date

2017-08-01

DOI

10.1002/acr.23121

Peer reviewed



Published in final edited form as:

Arthritis Care Res (Hoboken). 2017 August ; 69(8): 1179–1191. doi:10.1002/acr.23121.

THE ASSOCIATION BETWEEN BIOCHEMICAL MARKERS OF BONE TURNOVER AND BONE CHANGES ON IMAGING – DATA FROM THE OSTEOARTHRITIS INITIATIVE

Leticia A Deveza, MD¹, Virginia B Kraus, PHD², Jamie E Collins, PhD³, Ali Guermazi, PhD⁴, Frank W Roemer, MD^{4,5}, Michael Bowes, PhD⁶, Michael C Nevitt, PhD⁷, Christoph Ladel, PhD⁸, and David J Hunter, PhD¹

¹Rheumatology Department, Royal North Shore Hospital and Institute of Bone and Joint Research, Kolling Institute, University of Sydney, Sydney, NSW Australia

²Duke Molecular Physiology Institute and Division of Rheumatology, Duke University School of Medicine, Durham, NC, USA

³Orthopaedic and Arthritis Center for Outcomes Research, Department of Orthopaedic Surgery, Brigham and Women's Hospital, Boston, MA, USA

⁴Quantitative Imaging Center, Department of Radiology, Boston University School of Medicine, Boston, MA, USA

⁵Department of Radiology, University of Erlangen - Nuremberg, Erlangen, Germany

⁶Imorphics, Manchester, UK

⁷Department of Epidemiology and Biostatistics, University of California, San Francisco

⁸Merck KGaA, Darmstadt, Germany

Abstract

Objective—To determine the relationship between biochemical markers involved in bone turnover and bone features on imaging in knees with osteoarthritis (OA).

Methods—We analysed data from the OA Biomarkers Consortium within the Osteoarthritis Initiative (n=600). Bone marrow lesions (BMLs), osteophytes, subchondral bone area (mm²) and shape (position on 3D vector) were assessed on MRIs and bone trabecular integrity (BTI) was assessed on radiographs. Serum (s) and urinary (u) markers (sCTX-I, sNTX-I, uNTX-I, uCTX-II, uCTX-I alpha and beta) were measured. The associations between biochemical and imaging markers at baseline and over 24 months were assessed using regression models adjusted for covariates.

Results—At baseline, most biochemical markers were associated with BMLs, with c-statistics for the presence/absence of any BML ranging from 0.675 to 0.688. At baseline, uCTX-II was the

Corresponding author: Prof. Hunter at Rheumatology Department, Royal North Shore Hospital and Institute of Bone and Joint Research, Kolling Institute, University of Sydney, Sydney, NSW Australia. david.hunter@sydney.edu.au, Phone: 61 2 9463 1887 Fax: 61 2 9463 1077.

Potential conflict of interest: Leticia Deveza, David Hunter and Jamie Collins declare they have no conflict of interest.

marker most consistently associated with BMLs (odds of having 5 subregions affected compared to no BML increasing by 1.92-fold [95% CI 1.25, 2.96] per 1 SD of uCTX-II), large osteophytes (OR 1.39 [1.10, 1.77]), bone area and shape (highest partial R^2 0.032), and changes in bone shape over 24 months (partial R^2 from 0.008 to 0.024). Overall, biochemical markers were not predictive of changes in BMLs or osteophytes. Serum NTX-I was inversely associated with BTI of the vertical trabeculae (quadratic slope) in all analyses (highest partial R^2 0.028).

Conclusions—We found multiple significant associations, albeit most were weak. The role of systemic biochemical markers as predictors of individual bone anatomic features of single knees is limited based on our findings.

Keywords

osteoarthritis; biomarkers; biochemical marker; bone; magnetic resonance imaging

INTRODUCTION

Subchondral bone has been shown to play a pivotal role in the pathogenesis of osteoarthritis (OA) [1]. Changes in bone remodeling are frequently present early in the OA process and are associated with cartilage loss and further joint damage [2, 3]. Structural changes in the subchondral bone, such as bone marrow lesions (BMLs), variations in bone shape, area and trabecular texture have been associated with incident and progressive OA and are promising targets for interventions [1, 4]. In addition, BMLs are potentially reversible and were able to reflect the effects of interventions in previous trials [5, 6].

OA-related changes in the subchondral bone involve bone remodeling; it is intuitive that biochemical markers of bone turnover would also be altered in the presence of bone changes on imaging. Some biochemical markers have also been shown to be associated with OA presence, incidence and progression [7].

Developing a better understanding of the relationship between biochemical markers and MRI features may be advantageous for a number of reasons. Firstly, MRI is expensive and often not readily accessible; finding a blood or urine marker that corresponds to these MRI features might enable them to be deployed to enhance clinical trial efficiency or reduce costs. Secondly, if there is a biochemical marker that predicts change in a bone MRI feature that ultimately becomes a target of intervention, this would be helpful for screening and potential stratification of patient phenotypes in clinical trials. However, the minimally invasive nature may be a disadvantage of blood tests over non-contrast enhanced MRI, which is a non-invasive imaging technique.

Therefore, our aim was to assess whether systemic biochemical markers involved in bone remodeling are associated with presence of structural bone features on knee OA images, including BMLs, osteophytes, subchondral bone trabecular integrity (BTI), and subchondral bone shape and area. As a secondary aim, we examined the association between biochemical markers (baseline and time-integrated concentrations [TICs] over 24 months) and changes in imaging markers over 24 months. Our study population consisted of the 600 participants included in the OA Biomarkers Consortium study, a nested case-control study within the

Osteoarthritis Initiative (OAI) whose aim is to investigate biological markers involved in knee OA progression [8].

MATERIALS AND METHODS

The OAI is a multi-centre, longitudinal cohort which included 4,796 participants aged 45–79 years, with publicly accessible clinical, radiologic, and other data collected at baseline and at annual follow-up visits. We conducted an ancillary analysis of baseline and 24 months data from the Foundation for the National Institutes of Health (FNIH) Biomarkers Consortium within OAI [9].

Study participants

All 600 participants of the FNIH OA Biomarkers Consortium sample were included in our study. Eligible participants (one index knee per subject) were those with at least one knee with a Kellgren and Lawrence grade (KLG) of 1, 2 or 3 at baseline [10], assessed by central reading of standardized posterior-anterior weight-bearing radiographs, and availability of knee radiographs, knee MRI, stored biological specimens and clinical data at baseline and 24 months. Only knees with potential to meet criteria for radiographic and pain progression from baseline to 24 months were included (i.e. minimum medial joint space width 1.0 mm and/or WOMAC pain 91 on 0–100 scale at baseline). Additional criteria can be found at <https://oai.epi-ucsf.org/datarelease/FNIH.asp>.

Demographic and clinical data were assessed in all OAI participants at baseline. Baseline radiographs were acquired at the same time as baseline MRIs and read independently by two readers for KLG. Details of radiograph reading and MRI acquisition have been previously described [11].

Semi-quantitative MRI analysis of BML and osteophytes

BMLs were scored using the MOAKS (MRI Osteoarthritis Knee Score) method [12]. MOAKS uses a four-category ordinal scale to score BML size (grade 0: none; 1: <33% of subregional volume; 2: 33–66% of subregional volume; 3: >66% of subregional volume), which comprises both size of ill-defined and cystic components of BMLs in 15 subregions of the knee (5 subregions in the medial and lateral tibio-femoral compartments, 4 subregions in the patello-femoral compartment and tibial sub-spinous region which is associated with the insertion of the cruciate ligaments). The differentiation of cyst (well-delineated lesions with fluid equivalent signal) versus ill-defined BMLs is part of the MOAKS but was not taken into account in our analysis as only a minority of lesions were predominantly cystic (MOAKS scores 0 and 1) as opposed to ill-defined BMLs (10.4% of all BMLs at baseline).

We established the maximum BML size score for the joint as the highest BML grade (ranging from 0 to 3) across the whole knee and computed the total number of subregions affected by any BML (total score ranging from 0 to 15). We further categorized the number of subregions affected into 0, 1, 2, 3, 4 or 5, aiming to be consistent with the main, primary FNIH analysis [13].

MOAKS was also used to score osteophytes in 12 locations: patella (superior, inferior, medial and lateral), medial and lateral femur (anterior/trochlear, posterior and central) and central medial and lateral tibia. Similar to BMLs, osteophytes were scored according to size (0 = none; 1 = small; 2 = medium; 3 = large) in each subregion. For the analysis, osteophyte size was categorized as 0–1, 2 or 3, and the number of locations affected by any osteophyte across the entire knee was divided into 0–2, 3–5 or 6.

Quantitative analysis of bone area and vector of 3D shape

Active appearance models were used to segment the bone surfaces in medial and lateral femur, tibia and patella. The area of subchondral bone (tAB) was analysed in the medial and lateral compartments of femur and tibia (mm²). Bone shape was assessed by the position on three-dimensional (3D) bone shape vectors (normalized units: -1 is the mean shape of OA knees and +1 the mean shape for non-OA knees) in femur, tibia and patella. Details of the methods calculating the bone shape measurements can be found elsewhere [14–16].

Radiographic analysis for the assessment of BTI

The commercially available semi-automated KneeAnalyzer software (Optasia Medical, Manchester) was used to perform the radiographic fractal signature analyses of the medial tibia of knee radiographs to generate BTI parameters as previously described [17] with one modification. In slight contrast to our prior work, extraction of the BTI parameters for these analyses originated from the nadir (and center) of the fractal dimension curves to reduce the correlation between the estimated parameters. The advantage of this refinement has been to create near orthogonal (non-overlapping, independent) BTI parameters more suitable for multivariable and combinatorial statistical modeling allowing the researcher to assess which parameter was most related to the outcomes under study. The absolute values of the parameters are therefore not directly comparable to prior published work. To minimize confusion, all results are reported with reference to the horizontal or vertical filter from which they were generated. Fractal dimensions from which the BTI parameters were extracted reflect the number, spacing, and cross-connectivity of bone trabeculae. Among the 6 BTI parameters that were extracted, we included in our analysis the parameters that have been associated with OA status and progression in previous studies (i.e., quadratic slope from the horizontal and vertical filter [HF and VF, respectively] data and linear slope from the HF data) [17, 18].

Assessment of biochemical markers

Morning blood and second morning void urine specimens were collected at each visit after an overnight fast using a uniform protocol and sent to a commercial specimen repository where they were stored at -70°C. The results of the primary, main study analyses were reported in [19]. For the purpose of this study, we investigated the markers involved in bone turnover, namely serum (s) c-terminal crosslinked telopeptide of type I collagen (sCTX-I), urinary (u) CTX-I alpha and CTX-I beta, urinary c-terminal crosslinked telopeptide of type II collagen (uCTX-II) and serum and urinary type I collagen cross-linked N-telopeptide (sNTX-I and uNTX-I, respectively). Inter-plate coefficients of variation were low (3.0% to 7.6%).

We used an interpolated value from the standard curve extended from the lowest standard to zero if the concentration of the biochemical marker was below the lower limit of detection. For urine samples, we used creatinine-adjusted values obtained by dividing the urine assay values by the corresponding creatinine result for that sample. Technical information for each of the individual assay methods can be found in <https://oai.epi-ucsf.org/datarelease/>.

Definitions of change over time

We computed the maximum worsening in BML size scores and in osteophyte size scores across all subregions from baseline to 24 months and categorized it into no change, worsening by 1 grade or worsening by 2 grades for BMLs and no change or worsening for osteophytes. Within-grade changes (i.e., improvement or worsening) in BML size were also scored according to the MOAKS but were not considered in this analysis. Change in total number of subregions affected by any BML (grade >0) was calculated as the difference between the number of subregions affected at 24 months and baseline. This was categorized as improvement, no change, worsening by 1 subregion or worsening by 2 subregions for BMLs. The same method was used for subregions affected by any osteophyte and the result was categorized as no change or worsening.

Changes in tAB on the medial and lateral femur and tibia and in the position on 3D shape vectors for femur, tibia and patella were calculated as the difference between each parameter at 24 months and baseline. Time-integrated concentrations of BTI parameters and biochemical markers (area under the concentration versus 24 month time curve) were used to represent their change over 24 months in the longitudinal analysis.

Statistical analysis

The outcomes in our study were the structural features on bone imaging, namely presence and change of BMLs (maximum size and number of subregions affected), subchondral BTI, vector of 3D shape, tAB and osteophytes (maximum size and number of subregions affected). Biochemical markers were used as predictors. Continuous outcomes and biochemical marker concentrations were transposed to z scores prior to the analysis. Age, gender, body mass index (BMI), baseline KLG and use of medications with effect on bone (parathyroid hormone in the past 6 months and bisphosphonate in the past 12 months) were used as covariates. Multinomial logistic regression was used for ordinal outcomes (BML and osteophytes) and linear regression was used for continuous outcomes (BTI, vector of 3D shape and bone area). Odds ratio (OR) and 95% confidence interval (CI) for each 1 standard deviation (SD) increase in biochemical markers were used to assess strength of associations for BMLs and osteophytes, and partial R^2 and betas (95% CI) were used for BTI, tAB and vector of 3D shape.

We assessed the associations between: 1) biochemical and imaging markers at baseline (cross-sectional analysis), 2) baseline biochemical markers and changes in imaging features over 24 months (prognostic analysis) and 3) time-integrated concentrations (TICs) of biochemical markers over 24 months and changes in imaging features (concurrent analysis).

The diagnostic performance of biochemical markers to discriminate knees with any BML from the ones without BMLs (binary outcome) was evaluated using Receiver Operating

Characteristic (ROC) curve analysis. *P* values less than 0.05 were considered statistically significant. The software used was SPSS for Windows, version 22.0 (SPSS, Chicago, IL, USA).

RESULTS

The demographic characteristics of study participants and baseline concentrations of biochemical markers are described in Table 1. The majority of participants were women (58.8%), obese (mean BMI 30.7 kg/m²) and had a KLG 2 or 3 at baseline (87.5%).

Baseline imaging markers and their changes over 24 months are presented in the Supplementary Table 1. BMLs were found in 89% of participants at baseline and large lesions (grade 3) were present in 18.3% of knees. Over 24 months, BMLs increased in size by 1 grade and by 2 or more grades in 45.7% and 16.6%, of knees, respectively, and affected more subregions in 36.7%. Osteophytes most frequently affected 6 subregions at baseline and did not change in size or number in about 90%.

Cross-sectional analysis

Table 2 shows the associations between biochemical and bone imaging markers at baseline. Serum CTX-I and uCTX-I alpha were significantly associated with large BMLs (grade 3), with the odds of a large BML being present compared to no BML increasing by 1.47- and 1.48-fold, respectively, per 1 SD increase in each biochemical marker (95% CI: 1.04, 2.09 and 1.01, 2.15, respectively). Urinary CTX-II was associated with moderate and large (grades 2 and 3) BMLs in the unadjusted analysis (results not shown) but only reached statistical significance for grade 2 BMLs (OR 1.81 [95% CI 1.21, 2.74]) when covariates were added. All biochemical markers were associated with a higher number of subregions affected by any BML (4 and 5 subregions), except sNTX-1. Levels of uCTX-II were additionally associated with 2 and 3 subregions affected. Excluding the BMLs that were predominantly cysts from the analyses did not significantly affect the results (data not shown).

The area under the ROC curves (AUCs) using presence of any BML versus no BML as outcome, indicated the best diagnostic performance for uCTX-II, with an AUC of 0.613 (95% CI 0.542–0.685) before addition of covariates and 0.688 (95% CI 0.623–0.753) for the full model (Figure 1). Receiver Operating Characteristic curves using only moderate to large (grade 2 or 3) or large (grade 3) BMLs as outcome did not yield greater AUCs (results not shown).

Urinary CTX-II was the only biochemical marker associated with osteophytes, with the odds of having a grade 3 osteophyte compared to no osteophyte increasing by 1.39-fold per 1 SD increase in uCTX-II (95% CI 1.10, 1.77).

For BTI, baseline sNTX-I was inversely associated with the quadratic slope from the horizontal filter data (partial R² 0.025).

With respect to bone shape, uCTX-II was the soluble marker most consistently associated with this feature, with statistically significant associations with the femur, tibia and patella

3D shape vectors (partial R^2 ranging from 0.006 to 0.032). This marker, as well as sCTX-I, were associated with tAB in all joint locations studied in the adjusted analysis (partial R^2 ranging from 0.005 to 0.009), but not in the unadjusted analysis.

Prognostic analysis - Baseline biochemical markers and changes in bone imaging features over 24 months

Baseline uCTX-II was associated with changes in number of subregions affected by any BML, although this association was significant both for improvement and for worsening by 2 subregions or more. There was no association between baseline biochemical markers and changes in osteophytes over 24 months (Table 3).

Baseline values of sNTX-I were inversely associated with TICs of the quadratic slope from the BTI horizontal filter data, while sCTX-I was associated with TICs of the horizontal (linear slope) and vertical (quadratic slope) filter data.

Changes in position of 3D shape vectors towards an OA shape were associated with higher baseline levels of uCTX-II for the patellar and tibial bones (highest $R^2=0.012$ for patella). With respect to subchondral bone area, baseline sNTX-I was inversely associated with changes in tAB at the femur (medial and lateral) over 24 months.

Concurrent change analysis - TICs of biochemical markers and changes in bone imaging features over 24 months

Five hundred and eighty six participants had biochemical data available for all time points and were included in the concurrent analysis. There was a weak association between TIC of uCTX-II and an increase in the number of subregions affected by any BML by 2 or more subregions over 24 months (OR 1.35, 95%CI 1.03, 1.77) (Table 4). Similarly, TIC of uCTX-II was positively associated with increasing number of subregions affected by osteophytes (1.30 [95% CI 1.00, 1.68]) and TIC of sCTX-I was weakly associated with increasing osteophyte size.

For variations in subchondral BTI, TICs of sNTX-I and sCTX-I were inversely associated with the horizontal and vertical filter data, respectively. Time-integrated concentration of uCTX-II was associated with changes in bone shape at the femur, tibia and patella over 24 months and changed concurrently with tAB in all joint locations studied, except the lateral femur.

DISCUSSION

Both at baseline and longitudinally, we found several modest associations between collagen biochemical and bone imaging markers. In the cross-sectional analysis, higher baseline levels of most biochemical markers were associated with more subregions affected by BMLs across the whole knee; sCTX-I and uCTX-I alpha were also associated with larger BMLs. Fewer and less consistent associations were found for osteophytes, with only uCTX-II found associated with large osteophytes at baseline and increasing concurrently with increasing number of subregions affected over 24 months. Serum NTX-I was consistently associated with one BTI parameter (quadratic slope of the horizontal filter data) both at baseline and

over 24 months. Similarly, uCTX-II was consistently associated with 3D shape vectors in most joint locations in the cross-sectional and longitudinal analyses. In addition, higher baseline uCTX-II levels were associated with greater tAB in most joint locations at baseline and their TICs were associated with increases in tAB in the concurrent analysis.

The association between uCTX-II and BMLs is in accord with Garnero et al who also demonstrated a positive association between this marker and total BML score across the knee. No such relationship was found for sCTX-I [20]. In contrast to our investigation, BML was the only bone feature examined in that study. In addition, sNTX-I has been weakly associated with presence of BML on MRI, which was not observed in our study [21]. Although our main definition of BML magnitude and progression did not focus on total BML scores, we investigated if summing up the BML size scores across all 15 knee subregions both at baseline and at 24 months would reveal more evident associations at baseline or with BML progression. However, this approach showed similar results, with all biochemical markers, except sNTX-I, being associated with a total BML score in the highest quartile compared with the lowest quartile, and with the strongest association for uCTX-II (OR 1.81, 95% CI 1.32–2.50). No additional associations were found with BML progression.

Consistent with our findings, another study has shown that total osteophyte score, defined by the sum of osteophyte sizes in each knee compartment, was independently associated with baseline uCTX-II (a molecular marker of collagen type II degradation) but not with baseline uCTX-I alpha [22]. This association for uCTX-II may be consistent with the endochondral ossification related to osteophyte formation including expression of type II collagen in a cartilage anlage, with subsequent replacement by bone [23, 24].

Recent studies, however, have observed that uCTX-II is often associated with changes in bone on imaging, as well as with others soluble markers of bone remodeling [22, 25]. In our study, this marker was frequently associated with most of the bone imaging features investigated. CTX-II has been detected in the bone-cartilage interface [26] and it has been suspected that its origin is more related to bone than cartilage [25]. Interestingly, there is evidence that type II collagen and type II collagen metabolism are involved in bone marrow derived mesenchymal stem cell osteogenesis during bone remodeling and repair [27].

In the longitudinal analysis using either baseline or TIC values of biochemical markers, we found fewer significant associations for changes in BMLs and osteophytes over 24 months. Only a few studies have investigated this association longitudinally. Garnero et al showed a significant association between levels of uCTX-II in the highest tertile and worsening in BMLs after 3 months (relative risk=2.4; 95% CI 1.1, 5.0). In another study, uCTX-II and uCTX-1 alpha at baseline were predictive of osteophyte progression after 3 years ($p=0.0001$ and 0.01 , respectively) [22]. In our study, uCTX-II was not predictive of worsening in osteophyte number or size but changed concurrently with its progression over 24 months.

Previous work demonstrated that lower VF data of BTI, representing thickened horizontal trabeculae, was associated with higher risk of OA progression [17]. We found that, in the concurrent analysis, the quadratic slope of the VF data decreased concurrently with an

increase in sCTX-I levels, although this association was weak. Furthermore, sNTX-I was consistently associated with the horizontal filter data (vertical trabeculae) at baseline and over 24 months (inverse associations). Changes in BTI of the horizontal filter data was shown to be modestly associated with concurrent changes in both radiographic and MRI parameters of OA progression [18]. Higher horizontal filter data represents thinning of vertical trabeculae and, in our study, this was associated with lower sNTX-I levels. Variations in BTI probably occur due to altered subchondral bone turnover, which is reflected, in our study, by the significant associations with several markers of bone remodeling (baseline and TICs).

Three-D bone shape have been shown to identify knees at increased risk for incident radiographic OA [14]. Moreover, results from the FNIH Biomarkers study showed that changes in bone shape and area over 24 months were predictive of clinical and radiographic progression over 48 months [28]. There is a lack of studies determining their association with biochemical markers involved in bone remodeling and we showed that they were consistently associated with uCTX-II, particularly in the cross-sectional evaluation.

Our analyses were performed both with and without the inclusion of covariates including age, gender, BMI and KLG. It has been demonstrated that these demographic features and KLG may affect bone biochemical markers levels [29–32]. Moreover, they were often independently associated with the imaging markers in our study. It supports that these covariates may act as confounders in the association between bone biochemical markers and imaging features. We observed a considerable increase in the AUCs after the inclusion of the covariates, although most of the associations found were present both in the unadjusted and adjusted analyses.

There were several limitations in our study. First, we have performed a post-hoc analysis of the FNIH OA Biomarkers study, which was selected to include 1/4 OA progressors (both clinical and radiographic progression), 1/4 non-progressors and 1/2 either clinical only or radiographic only progressors. Case-control status has not been considered in our analysis and it is unclear if associations would be different in an unselected OA population with different rates of progression (e.g., general knee OA population). Second, we did not adjust for menopausal status, which is known to interfere with biochemical markers of bone turnover. However, the female population studied is comprised predominantly of postmenopausal women (86.6%), so it is unlikely that it would change the associations found. Third, we did not have data regarding bone mineral density (BMD) of participants to use as a covariate, which may influence the levels of biochemical markers of bone turnover. Finally, no adjustment was made for multiple comparisons so the presence of type I error cannot be ruled out.

In conclusion, despite several statistically significant associations, the practical utility of these systemic biochemical markers by themselves as predictors of these anatomic bone features of individual knees seems limited due to the modest strength of most of the associations.

Supplementary Material

Refer to Web version on PubMed Central for supplementary material.

Acknowledgments

We thank the Laboratory Analysts at LabCorp Clinical Trials, Li Cao and Des Delute who performed the biochemical analyses and Dr. David Hargrove who supervised the analyses.

Financial support: In-kind donations to support biochemical testing was provided by Alere Inc.; ARTIALIS S.A.; BioVendor - Laboratori medicina a.s.; IBEX Pharmaceuticals Inc.; Immunodiagnostic Systems Ltd; and Quidel Corporation.

Scientific and financial support for the FNIH OA Biomarkers Consortium and the study are made possible through grants, direct and in-kind contributions provided by: AbbVie; Amgen Inc.; Arthritis Foundation; Bioiberica S.A.; DePuy Mitek, Inc.; Flexion Therapeutics, Inc.; GlaxoSmithKline; Merck Serono; Rottapharm | Madaus; Sanofi; Stryker; The Pivotal OAI MRI Analyses (POMA) Study, NIH HHSN2682010000. We thank the Osteoarthritis Research Society International (OARSI) for their leadership and expertise on the FNIH OA Biomarker Consortium project. The OAI is a public-private partnership comprised of five contracts (N01-AR-2-2258; N01-AR-2-2259; N01-AR-2-2260; N01-AR-2-2261; N01-AR-2-2262) funded by the National Institutes of Health. Funding partners include Merck Research Laboratories; Novartis Pharmaceuticals Corporation, GlaxoSmithKline; and Pfizer, Inc. Private sector funding for the Consortium and OAI is managed by the FNIH.

Virginia Kraus has an issued patent related to BTI analysis but no related financial interests at this time. Ali Guermazi has received consulting fees from MerckSerono, Genzyme, OrthoTrophix, TissueGene, AstraZeneca and owns stock or stock options in Boston Imaging Core Lab (BICL), LLC. Frank Roemer owns stock or stock options in Boston Imaging Core Lab (BICL), LLC. Michael Bowes is employee of Imorphics Ltd, Kilburn House, Manchester Science Park, Manchester, M15 6SE, UK. Michael Nevitt receives grants from NIH and FNIH. Christoph Ladel is employee of Merck KGaA, Darmstadt, Germany.

REFERENCES

1. Funck-Brentano T, Cohen-Solal M. Subchondral bone and osteoarthritis. *Curr Opin Rheumatol*. 2015; 27:420–426. [PubMed: 26002035]
2. Hunter DJ, Zhang Y, Niu J, Goggins J, Amin S, LaValley MP, et al. Increase in bone marrow lesions associated with cartilage loss: a longitudinal magnetic resonance imaging study of knee osteoarthritis. *Arthritis Rheum*. 2006; 54:1529–1535. [PubMed: 16646037]
3. Crema MD, Felson DT, Roemer FW, Wang K, Marra MD, Nevitt MC, et al. Prevalent cartilage damage and cartilage loss over time are associated with incident bone marrow lesions in the tibiofemoral compartments: the MOST study. *Osteoarthritis Cartilage*. 2013; 21:306–313. [PubMed: 23178289]
4. Barr AJ, Campbell TM, Hopkinson D, Kingsbury SR, Bowes MA, Conaghan PG, et al. A systematic review of the relationship between subchondral bone features, pain and structural pathology in peripheral joint osteoarthritis. *Arthritis Res Ther*. 2015; 17:228. [PubMed: 26303219]
5. Pelletier JP, Roubille C, Raynauld JP, Abram F, Dorais M, Delorme P, et al. Disease-modifying effect of strontium ranelate in a subset of patients from the Phase III knee osteoarthritis study SEKOIA using quantitative MRI: reduction in bone marrow lesions protects against cartilage loss. *Ann Rheum Dis*. 2015; 74:422–429. [PubMed: 24297379]
6. Laslett LL, Doré DA, Quinn SJ, Boon P, Ryan E, Winzenberg TM, et al. Zoledronic acid reduces knee pain and bone marrow lesions over 1 year: a randomised controlled trial. *Ann Rheum Dis*. 2012; 71:1322–1328. [PubMed: 22355040]
7. van Spil WE, DeGroot J, Lems WF, Oostveen JC, Lafeber FP, et al. Serum and urinary biochemical markers for knee and hip-osteoarthritis: a systematic review applying the consensus BIPED criteria. *Osteoarthritis Cartilage*. 2010; 18:605–612. [PubMed: 20175979]
8. Nevitt MC, Felson DT, Lester G. The Osteoarthritis initiative: protocol for the cohort study. <http://oai.epi-ucsf.org/datarelease/docs/StudyDesignProtocol.pdf>.
9. Hunter DJ, Nevitt M, Losina E, Kraus V. Biomarkers for osteoarthritis: current position and steps towards further validation. *Best Pract Res Clin Rheumatol*. 2014; 28:61–71. [PubMed: 24792945]

10. Petersson IF, Boegård T, Saxne T, Silman AJ, Svensson B. Radiographic osteoarthritis of the knee classified by the Ahlback and Kellgren & Lawrence systems for the tibiofemoral joint in people aged 35–54 years with chronic knee pain. *Ann Rheum Dis.* 1997; 56:493–496. [PubMed: 9306873]
11. Wirth W, Hellio Le Graverand MP, Wyman BT, Maschek S, Hudelmaier M, Hitzl W, et al. Regional analysis of femorotibial cartilage loss in a subsample from the Osteoarthritis Initiative progression subcohort. *Osteoarthritis Cartilage.* 2009; 17:291–297. [PubMed: 18789729]
12. Hunter DJ, Guermazi A, Lo GH, Grainger AJ, Conaghan PG, Boudreau RM, et al. Evolution of semi-quantitative whole joint assessment of knee OA: MOAKS (MRI Osteoarthritis Knee Score). *Osteoarthritis Cartilage.* 2011; 19:990–1002. [PubMed: 21645627]
13. Collins JE, Losina E, Nevitt MC, Roemer FW, Guermazi A, Lynch JA, et al. Semi-Quantitative Imaging Biomarkers of Knee Osteoarthritis Progression: Data from the FNIH OA Biomarkers Consortium. *Arthritis Rheumatol.* 2016 [Epub ahead of print].
14. Neogi T, Bowes MA, Niu J, De Souza KM, Vincent GR, Goggins J, et al. Magnetic resonance imaging-based three-dimensional bone shape of the knee predicts onset of knee osteoarthritis: data from the osteoarthritis initiative. *Arthritis Rheum.* 2013; 65:2048–2058. [PubMed: 23650083]
15. Tamez-Peña JG, Farber J, González PC, Schreyer E, Schneider E, Totterman S. Unsupervised segmentation and quantification of anatomical knee features: data from the Osteoarthritis Initiative. *IEEE Trans Biomed Eng.* 2012; 59:1177–1186. [PubMed: 22318477]
16. Hunter D, Nevitt M, Lynch J, Kraus VB, Katz JN, Collins JE, et al. Longitudinal validation of periarticular bone area and 3D shape as biomarkers for knee OA progression? Data from the FNIH OA Biomarkers Consortium. *Ann Rheum Dis.* 2016; 75:1607–1614. [PubMed: 26483253]
17. Kraus VB, Feng S, Wang S, White S, Ainslie M, Brett A, et al. Trabecular morphometry by fractal signature analysis is a novel marker of osteoarthritis progression. *Arthritis Rheum.* 2009; 60:3711–3722. [PubMed: 19950282]
18. Kraus VB, Feng S, Wang S, White S, Ainslie M, Graverand MP, et al. Subchondral bone trabecular integrity predicts and changes concurrently with radiographic and magnetic resonance imaging-determined knee osteoarthritis progression. *Arthritis Rheum.* 2013; 65:1812–1821. [PubMed: 23576116]
19. Kraus VB, Collins JE, Hargrove D, Losina E, Nevitt M, Katz JN, et al. Predictive validity of biochemical biomarkers in knee osteoarthritis: data from the FNIH OA Biomarkers Consortium. *Ann Rheum Dis.* 2016 [Epub ahead of print].
20. Garnero P, Peterfy C, Zaim S, Schoenharting M. Bone marrow abnormalities on magnetic resonance imaging are associated with type II collagen degradation in knee osteoarthritis: a three-month longitudinal study. *Arthritis Rheum.* 2005; 52:2822–2829. [PubMed: 16145678]
21. Hunter DJ, Lavalley M, Li J, Bauer DC, Nevitt M, DeGroot J, et al. Biochemical markers of bone turnover and their association with bone marrow lesions. *Arthritis Res Ther.* 2008; 10:R102. [PubMed: 18759975]
22. Huebner JL, Bay-Jensen AC, Huffman KM, He Y, Leeming DJ, McDaniel GE, et al. Alpha C-telopeptide of type I collagen is associated with subchondral bone turnover and predicts progression of joint space narrowing and osteophytes in osteoarthritis. *Arthritis Rheumatol.* 2014; 66:2440–2449. [PubMed: 24909851]
23. Gelse K, Söder S, Eger W, Diemtar T, Aigner T. Osteophyte development--molecular characterization of differentiation stages. *Osteoarthritis Cartilage.* 2003; 11:141–148. [PubMed: 12554130]
24. Aigner T, Dietz U, Stöss H, von der Mark K. Differential expression of collagen types I, II, III, and X in human osteophytes. *Lab Invest.* 1995; 73:236–243. [PubMed: 7637324]
25. van Spil WE, Drossaers-Bakker KW, Lafeber FP. Associations of CTX-II with biochemical markers of bone turnover raise questions on its tissue origin: data from CHECK, a cohort study of early osteoarthritis. *Ann Rheum Dis.* 2013; 72:29–36. [PubMed: 22689318]
26. Bay-Jensen AC, Andersen TL, Charni-Ben Tabassi N, Kristensen PW, Kjaersgaard-Andersen P, Sandell L, et al. Biochemical markers of type II collagen breakdown and synthesis are positioned at specific sites in human osteoarthritic knee cartilage. *Osteoarthritis Cartilage.* 2008; 16:615–623. [PubMed: 17950629]

27. Chiu LH, Lai WF, Chang SF, Wong CC, Fan CY, Fang CL, et al. The effect of type II collagen on MSC osteogenic differentiation and bone defect repair. *Biomaterials*. 2014; 35:2680–2691. [PubMed: 24411332]
28. Hunter D, Nevitt M, Lynch J, Kraus VB, Katz JN, Collins JE, et al. Longitudinal validation of periarticular bone area and 3D shape as biomarkers for knee OA progression? Data from the FNIH OA Biomarkers Consortium. *Ann Rheum Dis*. 2016; 75:1607–1614. [PubMed: 26483253]
29. Maleki-Fischbach M, Jordan JM. New developments in osteoarthritis. Sex differences in magnetic resonance imaging-based biomarkers and in those of joint metabolism. *Arthritis Res Ther*. 2010; 12:212. [PubMed: 20701741]
30. Karsdal MA, Byrjalsen I, Bay-Jensen AC, Henriksen K, Riis BJ, Christiansen C. Biochemical markers identify influences on bone and cartilage degradation in osteoarthritis--the effect of sex, Kellgren-Lawrence (KL) score, body mass index (BMI), oral salmon calcitonin (sCT) treatment and diurnal variation. *BMC Musculoskelet Disord*. 2010; 11:125. [PubMed: 20565725]
31. Van Spil WE, Nair SC, Kinds MB, Emans PJ, Hilberdink WK, Welsing PM, et al. Systemic biochemical markers of joint metabolism and inflammation in relation to radiographic parameters and pain of the knee: data from CHECK, a cohort of early-osteoarthritis subjects. *Osteoarthritis Cartilage*. 2015; 23:48–56. [PubMed: 25205017]
32. Kraus VB, Hargrove DE, Hunter DJ, Renner JB, Jordan JM. Establishment of reference intervals for osteoarthritis-related soluble biomarkers: the FNIH/OARSI OA Biomarkers Consortium. *Ann Rheum Dis*. 2016 [Epub ahead of print].

SIGNIFICANCE AND INNOVATIONS

- The association between biochemical and imaging markers has not been well established in knee OA.
- We found that bone changes on imaging (i.e., bone marrow lesions, subchondral bone shape and area, osteophytes and bone trabecular integrity) were frequently associated with biochemical markers of bone turnover, indicating their relation with altered bone remodeling.
- CTX-II was the marker most consistently associated with bone imaging features.
- Based on the modest strength of associations, we do not strongly support the use of these biochemical markers as predictors for the presence of these bone imaging features in single knees.

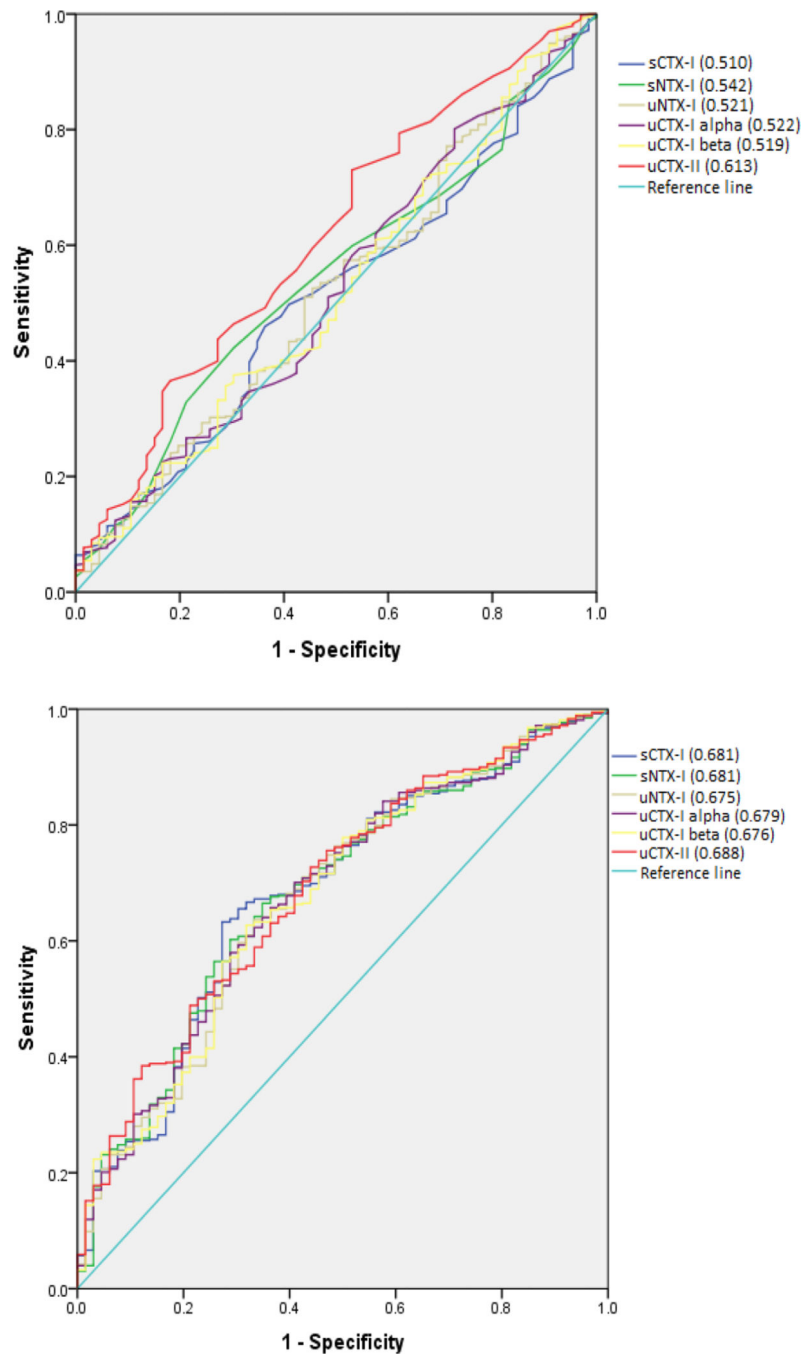


Figure 1. Receiver operating characteristic (ROC) curves of biochemical markers for predicting the presence of BML (BML > 0) at baseline. Top: unadjusted. Bottom: adjusted for covariates.

Table 1

Clinical and laboratorial characteristics of study participants at baseline (n=600).

Mean age (SD)	61.5 (8.9)
Female gender (%)	58.8
BMI (Kg/m²), mean (SD)	30.7 (4.8)
Right knee analyzed, n (%)	322 (53.7)
KLK at baseline, n (%)	
1	75 (12.5)
2	306 (51)
3	219 (36.5)
Race, n (%)	
White or Caucasian	475 (79.2)
Black or African American	109 (18.2)
Asian	5 (0.8)
Other non-white	11 (1.8)
Use of medications, n (%)	
Bisphosphonate (last year)	47 (7.8%)
PTH (last 6 months)	2 (0.3)
Biochemical markers (mean \pm SD) *	
uCTX-II (ug/mL)	0.30 \pm 0.19
uNTX-I (nmol BCE)	33.33 \pm 17.70
sNTX-I (nmol BCE)	15.11 \pm 5.21
sCTX-I (ng/mL)	0.39 \pm 0.21
uCTX-I alpha (ng/mL)	0.43 \pm 0.34
uCTX-I beta (ug/L)	2.26 \pm 1.76

* Non-transformed values.

KLK: Kellgren and Lawrence grade; PTH: Parathyroid hormone.

Table 2

Association between biochemical and imaging markers at baseline.

	sCTX-I	sNTX-I	uNTX-I	uCTX-II	uCTX-I alpha	uCTX-I beta
Maximum size	P=0.060	P=0.195	P=0.247	P=0.001	P=0.124	P=0.121
0	REF	REF	REF	REF	REF	REF
1	1.08 (0.78, 1.49)	1.08 (0.78, 1.51)	1.10 (0.78, 1.55)	1.29 (0.86, 1.95)	1.15 (0.80, 1.65)	1.14 (0.82, 1.60)
2	1.23 (0.89, 1.71)	1.28 (0.92, 1.79)	1.24 (0.88, 1.75)	1.83 (1.21, 2.74)[†]	1.27 (0.88, 1.82)	1.36 (0.97, 1.90)
3	1.47 (1.04, 2.09)[*]	1.30 (0.91, 1.85)	1.35 (0.94, 1.95)	1.51 (0.98, 2.33)	1.48 (1.01, 2.15)[*]	1.37 (0.96, 1.96)
N° of subregions	P=0.013	P=0.171	P=0.134	P=0.004	P=0.125	P=0.016
0	REF	REF	REF	REF	REF	REF
1	1.12 (0.79, 1.60)	1.29 (0.90, 1.85)	1.14 (0.78, 1.66)	1.09 (0.68, 1.73)	1.17 (0.79, 1.74)	1.19 (0.82, 1.73)
2	1.04 (0.73, 1.47)	1.03 (0.72, 1.48)	1.13 (0.78, 1.63)	1.58 (1.04, 2.40)[*]	1.21 (0.82, 1.78)	1.15 (0.80, 1.65)
3	1.06 (0.74, 1.51)	1.11 (0.78, 1.59)	1.11 (0.76, 1.60)	1.53 (1.00, 2.33)[*]	1.17 (0.79, 1.73)	1.08 (0.74, 1.56)
4	1.63 (1.14, 2.34)[†]	1.42 (0.99, 2.03)	1.46 (1.01, 2.13)[*]	1.79 (1.16, 2.77)[†]	1.52 (1.03, 2.24)[*]	1.62 (1.13, 2.34)[†]
5	1.47 (1.01, 2.15)[*]	1.34 (0.93, 1.93)	1.48 (1.01, 2.18)[*]	1.92 (1.25, 2.96)[†]	1.54 (1.03, 2.31)[*]	1.53 (1.05, 2.24)[*]
Maximum size	P=0.678	P=0.603	P=0.905	P=0.012	P=0.983	P=0.888
0-1	REF	REF	REF	REF	REF	REF
2	0.94 (0.76, 1.17)	0.95 (0.78, 1.15)	0.99 (0.80, 1.21)	1.02 (0.82, 1.26)	0.98 (0.79, 1.21)	0.95 (0.78, 1.16)
3	1.07 (0.81, 1.42)	0.87 (0.65, 1.15)	0.93 (0.69, 1.25)	1.39 (1.10, 1.77)[†]	0.99 (0.74, 1.32)	1.00 (0.77, 1.31)
N° of subregions	P=0.259	P=0.703	P=0.677	P=0.001	P=0.690	P=0.726
0-2	REF	REF	REF	REF	REF	REF
3-5	0.79 (0.59, 1.05)	0.89 (0.67, 1.18)	0.97 (0.72, 1.31)	0.68 (0.48, 0.96)[*]	0.91 (0.68, 1.23)	1.01 (0.76, 1.33)
6	0.88 (0.68, 1.15)	0.94 (0.72, 1.22)	1.07 (0.81, 1.41)	1.08 (0.81, 1.44)	1.01 (0.76, 1.33)	1.08 (0.83, 1.40)
Linear slope (HF)	0.001 / 0.029 (-0.062, 0.120)	0.002 / 0.050 (-0.035, 0.135)	0.000 / 0.011 (-0.092, 0.094)	0.000 / 0.000 (-0.086, 0.087)	0.000 / 0.003 (-0.088, 0.093)	0.000 / 0.023 (-0.069, 0.114)
Quadratic slope (HF)	0.001 / -0.035 (-0.127, 0.056)	0.025 / -0.165[‡] (-0.250, -0.081)	0.000 / 0.012 (-0.081, 0.106)	0.000 / -0.005 (-0.093, 0.082)	0.000 / -0.006 (-0.097, 0.085)	0.001 / -0.031 (-0.124, 0.061)
Quadratic slope (VF)	0.001 / -0.030 (-0.121, 0.061)	0.000 / -0.015 (-0.100, 0.070)	0.000 / 0.007 (-0.086, 0.101)	0.001 / 0.034 (-0.053, 0.121)	0.002 / -0.049 (-0.140, 0.042)	0.000 / 0.011 (-0.081, 0.103)

	sCTX-I	sNTX-I	uNIX-I	uCTX-II	uCTX-I alpha	uCTX-I beta
Vector						
Partial R² / Beta (95% CI)						
Femur	0.013 / -0.124[‡] (-0.198, -0.049)	0.003 / -0.059 (-0.129, 0.012)	0.002 / -0.051 (-0.126, 0.024)	0.032 / -0.188[‡] (-0.258, -0.117)	0.006 / -0.083[*] (-0.157, -0.009)	0.005 / -0.074[*] (-0.144, -0.002)
Tibia	0.001 / -0.040 (-0.115, 0.035)	0.000 / -0.006 (-0.084, 0.071)	0.001 / -0.030 (-0.113, 0.052)	0.016 / -0.135[‡] (-0.213, -0.056)	0.001 / -0.025 (-0.106, 0.057)	0.000 / -0.022 (-0.100, 0.056)
Patella	0.005 / -0.074 (-0.156, 0.008)	0.000 / -0.017 (-0.094, 0.060)	0.002 / -0.052 (-0.134, 0.030)	0.006 / -0.109[‡] (-0.188, -0.031)	0.004 / -0.069 (-0.151, 0.012)	0.001 / -0.034 (-0.112, 0.044)
Medial Femur	0.004 / 0.068[*] (0.012, 0.124)	0.001 / 0.037 (-0.016, 0.090)	0.000 / 0.013 (-0.043, 0.070)	0.009 / 0.101[‡] (0.048, 0.155)	0.000 / 0.014 (-0.042, 0.070)	0.000 / -0.005 (-0.059, 0.049)
Lateral Femur	0.003 / 0.062[*] (0.009, 0.114)	0.002 / 0.052[*] (0.002, 0.101)	0.000 / 0.000 (-0.053, 0.053)	0.006 / 0.085[‡] (0.034, 0.135)	0.000 / 0.009 (-0.043, 0.062)	0.000 / -0.009 (-0.059, 0.042)
Medial Tibia	0.005 / 0.075[‡] (0.024, 0.126)	0.001 / 0.038 (-0.010, 0.087)	0.000 / 0.019 (-0.033, 0.071)	0.005 / 0.075[‡] (0.026, 0.124)	0.001 / 0.025 (-0.026, 0.077)	0.000 / -0.004 (-0.053, 0.045)
Lateral Tibia	0.003 / 0.055[*] (0.002, 0.109)	0.002 / 0.041 (-0.009, 0.092)	0.000 / 0.006 (-0.060, 0.048)	0.005 / 0.075[‡] (0.023, 0.125)	0.000 / 0.004 (-0.050, 0.057)	0.000 / -0.009 (-0.060, 0.043)

Adjusted for covariates. Odds ratio and 95% confidence intervals (CI) are displayed for ordinal outcomes (BML and osteophytes) and partial R² and betas (95% CI) are displayed for continuous outcomes (BTI, vector of 3D shape and bone area).

Values in bold represent associations that were significant at p < 0.05.

* p < 0.05;

[‡] p < 0.01;

[‡] p < 0.001

Table 3

Association between baseline biochemical markers and changes in imaging features from baseline to 24 months.

	sCTX-I	sNTX-I	uNTX-I	uCTX-II	uCTX-I alpha	uCTX-I beta
Maximum size	P=0.387	P=0.869	P=0.833	P=0.905	P=0.682	P=0.999
No change	REF	REF	REF	REF	REF	REF
Worsening 1 subregion	1.10 (0.89, 1.35)	1.05 (0.86, 1.27)	1.06 (0.86, 1.31)	0.95 (0.78, 1.16)	1.09 (0.88, 1.35)	1.00 (0.82, 1.21)
Worsening 2+ subregions	0.93 (0.70, 1.22)	1.00 (0.78, 1.30)	1.02 (0.78, 1.34)	0.96 (0.74, 1.24)	1.06 (0.80, 1.39)	1.00 (0.78, 1.29)
BMLs						
N° of subregions	P=0.601	P=0.568	P=0.833	P=0.012	P=0.646	P=0.692
Improvement	1.18 (0.89, 1.56)	1.17 (0.89, 1.53)	1.03 (0.77, 1.37)	1.35 (1.04, 1.75)*	1.03 (0.78, 1.35)	1.09 (0.85, 1.40)
No change	REF	REF	REF	REF	REF	REF
Worsening 1 subregion	0.96 (0.77, 1.21)	1.03 (0.84, 1.26)	0.98 (0.78, 1.23)	1.02 (0.80, 1.29)	0.97 (0.77, 1.22)	0.92 (0.73, 1.15)
Worsening 2+ subregion	1.08 (0.79, 1.48)	0.90 (0.65, 1.24)	1.14 (0.84, 1.53)	1.46 (1.16, 1.92)†	1.19 (0.89, 1.60)	1.04 (0.78, 1.40)
Osteophyte						
Maximum size	P=0.462	P=0.818	P=0.798	P=0.620	P=0.738	P=0.959
No change	REF	REF	REF	REF	REF	REF
Worsening	0.91 (0.71, 1.16)	0.97 (0.77, 1.22)	0.96 (0.76, 1.23)	0.94 (0.74, 1.19)	0.95 (0.75, 1.22)	0.99 (0.79, 1.24)
N° of subregions						
No change	P=0.803	P=0.522	P=0.868	P=0.720	P=0.974	P=0.920
Worsening	1.03 (0.77, 1.39)	0.90 (0.66, 1.23)	1.02 (0.76, 1.37)	0.94 (0.67, 1.30)	1.00 (0.74, 1.34)	0.98 (0.73, 1.31)
Linear slope (HF)						
	0.007 / 0.096* (0.004, 0.188)	0.005 / 0.074 (-0.012, 0.159)	0.005 / 0.084 (-0.011, 0.180)	0.003 / 0.063 (-0.027, 0.152)	0.011 / 0.117* (0.023, 0.210)	0.006 / 0.090 (-0.003, 0.183)
Quadratic slope (HF)						
	0.001 / -0.035 (-0.128, 0.059)	0.023 / -0.158‡ (-0.244, -0.072)	0.001 / 0.028 (-0.069, 0.125)	0.000 / 0.014 (-0.077, 0.104)	0.000 / 0.003 (-0.093, 0.098)	0.000 / 0.007 (-0.087, 0.102)
Quadratic slope (VF)						
	0.010 / -0.114* (-0.202, -0.021)	0.003 / -0.052 (-0.138, 0.035)	0.001 / -0.033 (-0.130, 0.064)	0.002 / -0.043 (-0.134, 0.047)	0.002 / -0.050 (-0.145, 0.045)	0.003 / -0.060 (-0.155, 0.034)
Vector						
Femur	0.000 / 0.024 (-0.064, 0.112)	0.001 / 0.037 (-0.046, 0.119)	0.000 / 0.013 (-0.074, 0.101)	0.000 / -0.023 (-0.109, 0.062)	0.000 / 0.024 (-0.063, 0.111)	0.000 / 0.015 (-0.068, 0.098)
Tibia	0.001 / -0.013 (-0.102, 0.076)	0.004 / -0.069 (-0.152, 0.015)	0.001 / -0.031 (-0.120, 0.058)	0.008 / -0.094* (-0.179, -0.009)	0.002 / -0.054 (-0.141, 0.034)	0.000 / -0.016 (-0.101, 0.068)

	sCTX-I	sNTX-I	uNTX-I	uCTX-II	uCTX-I alpha	uCTX-I beta
Patella	0.003 / -0.063 (-0.151, 0.026)	0.001 / -0.036 (-0.119, 0.047)	0.011 / -0.078 (-0.166, 0.011)	0.012 / -0.116[†] (-0.201, -0.031)	0.008 / -0.099[*] (-0.186, -0.011)	0.002 / -0.047 (-0.131, 0.037)
Medial Femur	0.001 / 0.032 (-0.056, 0.121)	0.009 / -0.099[*] (-0.182, -0.017)	0.002 / 0.052 (-0.035, 0.140)	0.002 / 0.047 (-0.039, 0.131)	0.001 / 0.034 (-0.054, 0.121)	0.001 / 0.026 (-0.058, 0.109)
Lateral Femur	0.000 / 0.023 (-0.066, 0.112)	0.016 / -0.131[‡] (-0.213, -0.047)	0.000 / -0.001 (-0.090, 0.087)	0.001 / -0.036 (-0.121, 0.049)	0.000 / -0.003 (-0.091, 0.085)	0.001 / -0.034 (-0.118, 0.050)
Medial Tibia	0.003 / 0.062 (-0.028, 0.152)	0.001 / -0.027 (-0.012, 0.057)	0.003 / 0.062 (-0.027, 0.152)	0.006 / 0.081 (-0.005, 0.167)	0.006 / 0.084 (-0.005, 0.172)	0.001 / 0.040 (-0.045, 0.125)
Lateral Tibia	0.006 / 0.086 (-0.003, 0.175)	0.004 / -0.069 (-0.152, 0.015)	0.010 / 0.111[*] (0.022, 0.198)	0.014 / 0.124[†] (0.039, 0.209)	0.013 / 0.128[†] (0.034, 0.214)	0.004 / 0.070 (-0.014, 0.154)

Adjusted for covariates; and respective baseline imaging feature. Odds ratio and 95% confidence intervals (CI) are displayed for ordinal outcomes (BML and osteophytes) and partial R² and betas (95% CI) are displayed for continuous outcomes (BTI, vector of 3D shape and bone area).

Values in bold represent associations that were significant at p < 0.05.

* p < 0.05;

[†] p < 0.01;

[‡] p < 0.001

Table 4
 Concurrent changes in biochemical markers and imaging features from baseline to 24 months

	sCTX-I	sNTX-I	uNTX-I	uCTX-II	uCTX-I alpha	uCTX-I beta
Maximum size worsening	P=0.740	P=0.666	P=0.414	P=0.262	P=0.399	P=0.947
No change	REF	REF	REF	REF	REF	REF
Worsening by 1 grade	1.08 (0.88, 1.32)	1.03 (0.84, 1.25)	0.82 (0.42, 1.60)	1.16 (0.94, 1.43)	0.67 (0.08, 5.35)	1.00 (0.82, 1.22)
Worsening by 2+ grades	1.04 (0.80, 1.35)	1.11 (0.87, 1.42)	0.85 (0.43, 1.68)	0.88 (0.71, 1.09)	0.88 (0.54, 1.45)	1.04 (0.80, 1.34)
BML						
OR (95% CI)	P=0.990	P=0.773	P=0.662	P=0.162	P=0.726	P=0.994
N° of subregions						
Improvement	0.98 (0.75, 1.30)	1.03 (0.77, 1.37)	0.49 (0.07, 3.54)	1.15 (0.87, 1.51)	0.62 (0.02, 14.19)	0.98 (0.74, 1.29)
No change	REF	REF	REF	REF	REF	REF
Worsening by 1 subregion	1.03 (0.83, 1.27)	1.05 (0.86, 1.28)	0.90 (0.56, 1.47)	1.05 (0.81, 1.36)	0.86 (0.36, 1.02)	1.01 (0.82, 1.25)
Worsening by 2+ subregions	1.01 (0.74, 1.39)	0.87 (0.62, 1.23)	0.90 (0.44, 1.80)	1.35 (1.03, 1.77)*	0.89 (0.43, 1.87)	0.98 (0.71, 1.34)
Osteophyte						
OR (95% CI)	P=0.46	P=0.085	P=0.759	P=0.675	P=0.739	P=0.054
No change	REF	REF	REF	REF	REF	REF
Worsening	1.25 (1.00, 1.56)*	1.20 (0.97, 1.48)	0.959 (0.70, 1.30)	1.04 (0.84, 1.29)	0.928 (0.59, 1.43)	1.24 (0.99, 1.55)
N° of subregions affected						
OR (95% CI)	P=0.668	P=0.902	P=0.834	P=0.061	P=0.907	P=0.973
No change	REF	REF	REF	REF	REF	REF
Worsening	1.06 (0.79, 1.42)	0.98 (0.72, 1.33)	0.92 (0.37, 2.31)	1.30 (1.00, 1.68)*	0.96 (0.52, 1.78)	1.00 (0.74, 1.35)
BTI						
OR (95% CI)						
Linear slope (HF)	0.001 / 0.034 (-0.052, 0.119)	0.005 / 0.073 (-0.010, 0.156)	0.000 / 0.006 (-0.074, 0.087)	0.001 / 0.033 (-0.054, 0.121)	0.000 / 0.004 (-0.077, 0.085)	0.001 / 0.040 (-0.049, 0.129)
Quadratic slope (HF)	0.000 / -0.022 (-0.108, 0.064)	0.028 / -0.167[‡] (-0.250, -0.084)	0.006 / 0.076 (-0.005, 0.158)	0.005 / 0.075 (-0.013, 0.164)	0.006 / 0.075 (-0.006, 0.157)	0.000 / -0.005 (-0.095, 0.085)
Quadratic slope (VF)	0.008 / -0.090* (-0.176, -0.004)	0.002 / -0.040 (-0.124, 0.044)	0.001 / -0.026 (-0.108, 0.056)	0.003 / -0.056 (-0.145, 0.032)	0.001 / -0.023 (-0.105, 0.058)	0.004 / -0.070 (-0.159, 0.020)
Vector						
OR (95% CI)	0.001 / -0.037 (-0.121, 0.047)	0.000 / -0.008 (-0.090, 0.075)	0.000 / -0.013 (-0.093, 0.067)	0.024 / -0.167[‡] (-0.251, -0.083)	0.000 / -0.012 (-0.092, 0.067)	0.002 / -0.046 (-0.130, 0.038)

	sCTX-I	sNTX-I	uNTX-I	uCTX-II	uCTX-I alpha	uCTX-I beta
Tibia	0.000 / 0.007 (-0.078, 0.092)	0.004 / -0.065 (-0.150, 0.018)	0.000 / -0.019 (-0.100, 0.063)	0.014 / -0.126[‡] (-0.211, -0.039)	0.000 / -0.020 (-0.102, 0.061)	0.000 / -0.016 (-0.147, 0.124)
Patella	0.004 / -0.067 (-0.152, 0.018)	0.002 / -0.043 (-0.127, -0.041)	0.004 / -0.062 (-0.143, 0.019)	0.024 / -0.164[‡] (-0.248, -0.079)	0.004 / -0.061 (-0.141, 0.020)	0.003 / -0.061 (-0.146, 0.025)
Medial Femur	0.002 / 0.053 (-0.032, 0.137)	0.007 / -0.089[*] (-0.127, -0.041)	0.000 / -0.008 (-0.088, 0.072)	0.017 / 0.138[‡] (0.054, 0.223)	0.000 / -0.011 (-0.090, 0.069)	0.003 / 0.060 (-0.025, 0.144)
Lateral Femur	0.001 / 0.037 (-0.049, 0.122)	0.016 / -0.130[‡] (-0.213, 0.046)	0.001 / 0.036 (-0.045, 0.116)	0.005 / 0.075 (-0.012, 0.160)	0.001 / 0.036 (-0.045, 0.116)	0.000 / -0.017 (-0.102, 0.068)
Medial Tibia	0.000 / 0.016 (-0.070, 0.103)	0.002 / -0.045 (-0.130, 0.039)	0.000 / -0.009 (-0.090, 0.073)	0.016 / 0.134[‡] (0.048, 0.220)	0.000 / -0.007 (-0.088, 0.075)	0.002 / 0.044 (-0.042, 0.130)
Lateral Tibia	0.003 / 0.059 (-0.027, 0.144)	0.006 / -0.078 (-0.162, 0.006)	0.000 / 0.020 (-0.062, -0.100)	0.024 / 0.164[‡] (0.079, 0.249)	0.000 / 0.018 (-0.069, 0.200)	0.006 / 0.084 (-0.002, 0.168)

Adjusted for covariates and respective baseline imaging feature. Odds ratio and 95% confidence intervals (CI) are displayed for ordinal outcomes (BML and osteophytes) and partial R² and betas (95% CI) are displayed for continuous outcomes (BTI, vector of 3D shape and bone area).

Values in bold represent associations that were significant at p < 0.05.

* p < 0.05;

[‡] p < 0.01;

^{‡‡} p < 0.001